An *in vitro* system for the study of ultrasound contrast agents using a commercial imaging system

2001 Phys. Med. Biol. 46 3301

(http://iopscience.iop.org/0031-9155/46/12/316)

INSTITUTE OF PHYSICS PUBLISHING PHYSICS IN MEDICINE AND BIOLOGY

Phys. Med. Biol. **46** (2001) 3301–3321 PII: S0031-9155(01)22476-2

An *in vitro* system for the study of ultrasound contrast agents using a commercial imaging system

V Sboros[1], C M Moran[1], T Anderson[1], L Gatzoulis[1], A Criton[2], M Averkiou[2], S D Pye[1] and W N McDicken[1]

[1]Department of Medical Physics and Medical Engineering, Royal Infirmary of Edinburgh, University of Edinburgh, 1 Lauriston Place, Edinburgh, EH3 9YW, UK
[2]Advanced Technology Laboratories, Bothell, WA, USA

E-mail: Vassilis.Sboros@ed.ac.uk

Received 2 March 2001, in final form 21 August 2001
Published 14 November 2001
Online at stacks.iop.org/PMB/46/3301

Abstract

An *in vitro* system for the investigation of the behaviour of contrast microbubbles in an ultrasound field, that provides a full diagnostic range of settings, is yet to be presented in the literature. The evaluation of a good compromise of such a system is presented in this paper. It is based on (a) an HDI3000 ATL scanner (Bothell, WA, USA) externally controlled by a PC and (b) on the use of well-defined reference materials. The suspensions of the reference ultrasonic scattering material are placed in an anechoic tank. The pulse length ranges from 2 to 10 cycles, the acoustic pressure from 0.08 to 1.8 MPa, the transmit frequency from 1 to 4.3 MHz, and the receive frequency from 1 to 8 MHz. The collection of 256 samples of RF data, at an offset distance from the transducer face, was performed at 20 MHz digitization rate, which corresponds to approximately 1 cm depth in water. Two particle suspensions are also presented for use as reference scatterers for contrast studies: (a) a suspension of Orgasol® (ELF Atochem, Paris, France) particles ($\sim$5 μm mean diameter) and (b) a suspension of Eccosphere® (New Metals & Chemicals Ltd, Essex, UK) particles ($\sim$50 μm mean diameter). A preliminary experiment with the contrast agent Definity (DuPont Pharmaceutical Co, Waltham, MA) showed that the above two materials are suitable for use as a reference for contrast backscatter.

(Some figures in this article are in colour only in the electronic version)

1. Introduction

The introduction of contrast agents in the field of diagnostic ultrasound was followed by the discovery that the interaction between the ultrasound beam and the contrast microbubbles was a complicated one. The incident ultrasound beam was shown to induce non-linear bubble motion (de Jong *et al* 1991, Schrope *et al* 1992, Schrope and Newhouse 1993, Burns *et al* 1994), as well as destroying the bubbles (Porter *et al* 1995, Porter and Xie 1996). A full

understanding of the complicated interaction between the microbubbles and ultrasound is a prerequisite in assessing the true potential of ultrasound contrast imaging. In order to build a successful model which describes that interaction, sufficient experimental data have to be accumulated. *In vitro* experiments performed in parallel with theoretical modelling of the behaviour of Albunex microbubbles in the ultrasound field, initiated a systematic investigation of the behaviour of contrast microbubbles (de Jong *et al* 1992, 1994a, 1994b, de Jong and Hoff 1993). The properties of newer agents in various acoustic fields have been reported (Chang *et al* 1996, Krishna and Newhouse 1997, Frinking and de Jong 1998, Frinking *et al* 1999), and the visualization of the behaviour of microbubbles in the ultrasound field was greatly assisted using optical microscopy (Morgan *et al* 1998, Dayton *et al* 1999). The non-linearity of the bubble motion in the ultrasound field and the calculation of the production of harmonic components was simulated by Chin and Burns (1997). This model remains to be tested. However, an experimental set-up that can cover a wide range of settings (e.g. transmit frequency, acoustic pressure, pulse length) similar to those used in diagnostic ultrasound applications is yet to be reported. The aim of this paper is to introduce such a set-up and evaluate it.

In a previous communication an *in vitro* experimental set-up was introduced (Sboros *et al* 2000a). It was later used to assess the lifetime of contrast agents in suspension, the decay when the suspension was degassed and also the relationship between backscatter and bubble concentration (Sboros *et al* 2000b). This system was useful in assessing some basic properties of contrast agents, but it is limited due to its scanner limitations. The transmit frequencies were fixed to the central frequency of each transducer (3 MHz for the quoted papers) and only the acoustic pressure could be altered. An experimental set-up designed to assess the acoustic properties of contrast agents should ideally provide a wide range of beam settings with respect to frequency (0.01–20 MHz), acoustic pressure (0.01–3 MPa), and pulse length (1–10 cycles). Ideally each should be changed independently. This would allow a rigorous assessment of the acoustical properties of different agents and consequently specify the settings for optimal imaging. Subsequently, the assessment of the fundamental and harmonic components, generated by the microbubble non-linear oscillation and received in the backscatter signal, would provide valuable knowledge on the complexity of the interaction of the microbubbles with the ultrasonic field.

Unfortunately transducer technology limitations alone provide an obstacle to achieving those goals. The spectral sensitivity of transducers has to date been the major limitation and in order to obtain results over the whole scattered spectrum the solution to date has been to use more than one transducer (de Jong *et al* 1993).

This paper introduces an ultrasound system that is a reasonable compromise for the ideal system described above. It is based on an HDI3000 ATL scanner (Advanced Technology Laboratories, Bothell, WA, USA), which provides wide and flexible external control of frequency, acoustic pressure and pulse length. The most rapid area of technological advance is in medical ultrasound equipment. Single element transducer technology is not generally tailored to medical ultrasound applications and competition is not as prominent as in the medical ultrasound equipment. The use of a commercial scanner will lead to an ever-improving *in vitro* set-up compared to a system built in the lab and based on single element transducers.

2. Materials and methods

2.1. The set-up

Figure 1 illustrates the experimental set-up. Various suspensions of particles were insonated in an anechoic tank (Sboros *et al* 2000a) using an HDI3000 ATL scanner, which was connected

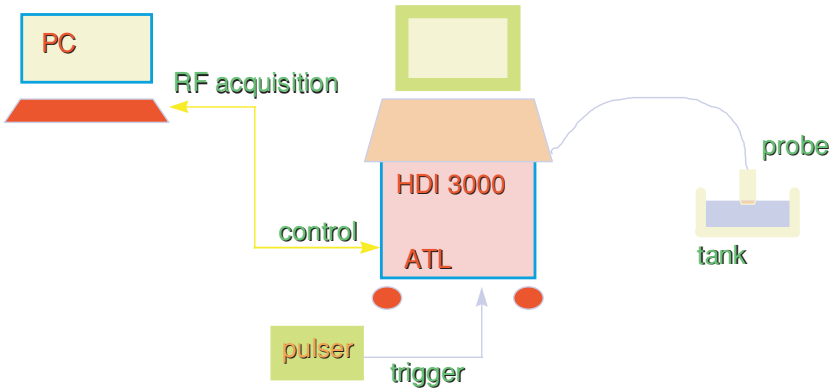

Figure 1. The experimental set-up. Suspensions of particles were insonated using an HDI3000 ATL scanner, which was controlled by a PC. A pulse generator was connected to the ECG lead in order to acquire triggered frames. Data were stored in the PC for processing and analysis.

to a PC through its serial port. In addition, the ECG lead was connected to a pulse generator (Phillips PM5705) in order to trigger frames at different time intervals. The pulses generated and transmitted to the ECG lead were 1 ms in duration, had 0.5 Hz repetition frequency and 5 V amplitude.

The tank used in the experiments was lined with an acoustic absorber (CERAM AB, Lund, Sweden) which for 3 MHz ultrasound produces an echo 32 dB below that of a perfect reflector. The size of the tank was 10 cm high × 15 cm long × 7 cm wide and it was made from Perspex (plexiglass). The distance of the scanning surface of the ultrasound imaging probe from the bottom of the tank was fixed at 6 cm.

2.1.1. The scanner and the controlling set-up. The scanner provided a large range of settings. The combined transmit frequency range for the two-phased array probes (P3-2 and P5-3) was 1.17–4.28 MHz and each could provide a mechanical index (MI) range of 0.1–0.7 (as displayed on the monitor) and a pulse length range of 2–10 cycles. The different ultrasound fields were controlled by the PC using Labview 5.1 graphical programming software (National Instruments, Austin, Texas, USA). The programs were supplied by ATL and were appropriately modified for the purposes of these experiments. With this software, it was possible to control the transmit frequency, the pulse length, the focal range and the offset position of the region of interest (ROI).

The digitization rate of the scanner was 20 MHz and the number of data points acquired was 256 for each line, which is equivalent to 1 cm depth. This information was acquired for 96 lines in each frame. Therefore the acquired ROI for a frame was 96 lines wide, 1 cm long beginning at 4 cm from the probe. After setting the scanner at 'freeze', a buffer temporarily stored the previous 90 frames.

Calibration of the scanner was performed using a PVDF needle hydrophone with 0.2 mm diameter (Precision Acoustics Ltd, Dorchester, UK) calibrated by the National Physical Laboratory (Teddington, UK).

The centre frequency and the bandwidth at 6 dB down from the peak amplitude of the transmitted pulse in the frequency domain were measured at 4.5 cm from the probe for all the different ultrasound fields generated by the scanner using a spectrum analyser (TF2370, Marconi Instruments Ltd, St Albans, UK). All the transmitted pulses at different pulse lengths, acoustic pressures and transmit frequencies were visually inspected in the

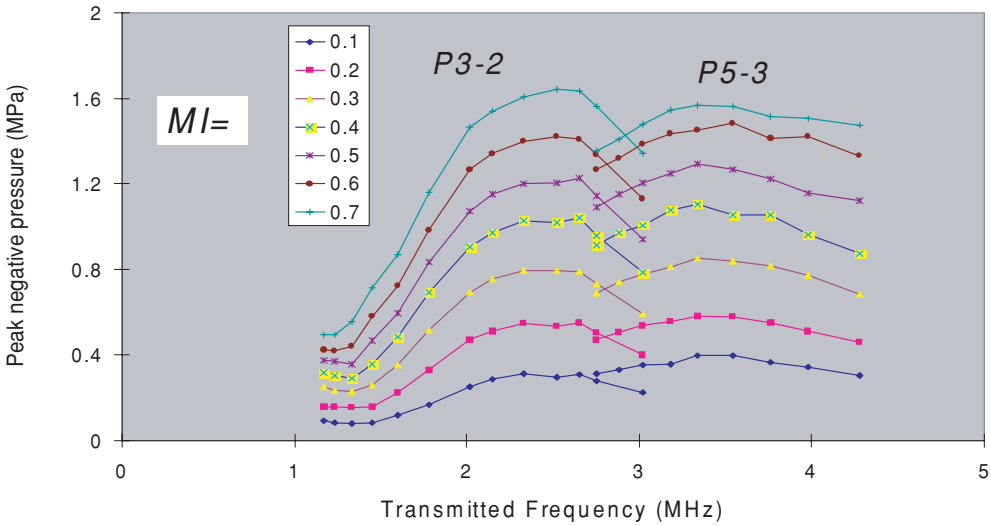

Figure 2. Calibration of the HDI3000 using a PVDF needle hydrophone. The pulse length was 6 cycles. The frequency ranged from 1.17 to 3.02 MHz for the P3-2 probe and from 2.75 to 4.28 MHz for the P5-3 probe. The peak negative pressure, measured at 4.5cm from the probe, was plotted against frequency and was grouped in the seven different MI settings ranging from 0.1 to 0.7. The MI values are not the true MI, but those displayed on the monitor of the scanner. The overall uncertainty of the hydrophone measurement, as specified by the National Physical Laboratory, is ±8%.

display of the spectrum analyser, and those that did not provide a satisfactory bell-shaped spectrum and a distinct centre frequency were not used in the experiments. These data were input to a statistical programme and run in the SAS statistical software (SAS Institute, Cary, NC), available in the University of Edinburgh network, in order to model the bandwidth as a function of the frequency and the pulse length. The outcome provided the equation

$$bw = 0.072 + 0.969\, f/cy \tag{1}$$

where bw is the bandwidth at 6 dB down from the peak amplitude, f the centre frequency in MHz, and cy the number of cycles in a pulse. The regression coefficient was 0.98. This relationship would be expected as a result of the Fourier transformation theory. Short pulses or/and higher frequency signals provide larger bandwidth signals.

Figure 2 illustrates the calibration of acoustic pressure of the scanner, using the hydrophone at a 6-cycle pulse length. The peak negative pressure measured at 4.5 cm was plotted against frequency. The different graphs show the calibration at different MIs, ranging from 0.1 to 0.7. The frequency ranged from 1.17 to 3.02 MHz for the P3-2 probe and from 2.75 to 4.28 MHz for the P5-3. The sensitivity peaked at 2.52 MHz for the P3-2 probe and at 3.54 MHz for the P5-3.

2.1.2. The data acquisition. Data could be acquired from the buffer of the scanner using another Labview program. This program was also supplied by ATL and modified for the purposes of the experiments. It was possible to acquire any part of the data available in the buffer. The data were saved in an ASCII format in the hard disc of the PC.

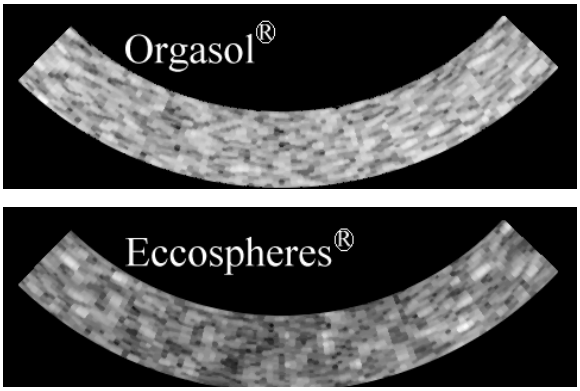

Figure 3. Image-reconstructed RF data for the water suspension of Orgasol® and the gelatine suspension of Eccosphere®. Frequency = 2 MHz, MI = 0.5 and cycles = 2.

2.2. The data processing

2.2.1. Image reconstruction. The collected data were in 96 lines × 256 points format. The IDL 5.0.2 programming software (Research Systems, Boulder, Colorado, USA) was used to reconstruct the image data. No interpolation was used to reconstruct the images. The algorithm was developed in the Department of Medical Physics. Typical images are displayed in figure 3. The image reconstruction was primarily used for visual inspection of the data for artefacts.

2.2.2. Backscatter calculations. The backscatter information was extracted from the RF data using a Matlab (Mathworks, Natick, MA) program. The data were digitally filtered with elliptic band-pass filters with the following characteristics:

(a) 14th order, 0.01 dB passband ripple width and 70 dB stopband loss to remove the DC offset,
(b) 7th order, 0.01 dB passband ripple width and 70 dB stopband loss, to filter out the fundamental, and
(c) 8th order, 0.01 dB passband ripple width and 70 dB stopband loss, to filter out the 2nd or 3rd harmonic.

The window used for the first filter was from 600 kHz to 9 MHz, while for the rest it was centred at the corresponding frequency and was 1 MHz wide.

After the data have been filtered appropriately, a Hilbert transform was applied and the average square was calculated. This provided the backscatter intensity at the particular spectral component (either the whole RF signal, or fundamental, 2nd, 3rd harmonic). The backscatter intensity has an arbitrary unit system as this is set by the digitizing process of the scanner.

2.2.3. Normalized backscatter calculation. Because of the increased control of the ultrasonic beam shape, due to the range of available settings, a variety of beam shapes can be achieved. To exclude the effects of beam-shape on the measurements, a normalization procedure was adopted where using suitable reference materials a satisfactory analysis of the backscatter information from contrast agents could be achieved. Using a reference material of a similar nature to normalize the investigated material has proven to be more accurate than the usual substitution technique where the measurements from a non-focused transducer are normalized

with respect to the echo of a flat reflector (Wang and Shung 1997). Wang and Shung showed that by using a reference material the transducer effects could be virtually eliminated and the calculation of the backscatter coefficient under investigation made easier. In the present study the normalizing technique is taken a step further by using the information in different spectral domains of the signal from both contrast and reference media.

The average backscatter intensity of the data frames from the agent were normalized by means of the backscatter of two other imaging materials (Sboros *et al* 2000a). Sboros *et al* define normalized backscatter as a unitless physical quantity similar to the integrated backscatter, calculated by the ratio of the backscatter intensity under investigation to that of a reference material. In principle, normalization was considered essential for contrast studies in order to:

(a) compensate for the changes in the beam shape (at different settings) including those caused by non-linear propagation, and
(b) provide a comparison with a linearly scattering material of similar particle density and size distribution.

In the present study each one of the four spectral intensity components of the agent (derived by the filtering process) was divided by the same components of one of the solid particle suspensions to form the normalized backscatter intensity at the particular acoustic frequency window. This adds a new dimension to the conventional normalization process whereby the average backscatter intensity of a suspension of linear scatterers (Wang and Shung 1997), or a suspension of contrast (Sboros *et al* 2000a) was normalized using another suspension of linear scatterers.

If we define the overall intensity as the sum of all the harmonic (including subharmonics and ultraharmonics) intensity components then,

$$I_{\text{contrast}} = I^{(1)}_{\text{contrast}} + I^{(2)}_{\text{contrast}} + I^{(3)}_{\text{contrast}} + \cdots \tag{2}$$

where I_{contrast}, $I^{(1)}_{\text{contrast}}$, $I^{(2)}_{\text{contrast}}$ and $I^{(3)}_{\text{contrast}}$ are the overall backscatter intensity and the individual intensities of the fundamental, 2nd and 3rd harmonic, respectively, for the contrast agent frames, and also

$$I_{\text{ref}} = I^{(1)}_{\text{ref}} + I^{(2)}_{\text{ref}} + I^{(3)}_{\text{ref}} + \cdots \tag{3}$$

where I_{ref}, $I^{(1)}_{\text{ref}}$, $I^{(2)}_{\text{ref}}$ and $I^{(3)}_{\text{ref}}$ are the overall backscatter intensity and the individual intensities of the fundamental, 2nd and 3rd harmonic, respectively, for the reference suspension of linear scatterers, it is evident that:

$$\frac{I_{\text{contrast}}}{\mathrm{I}_{\text{ref}}} \neq \frac{\mathrm{I}^{(1)}_{\text{contrast}}}{I^{(1)}_{\text{ref}}} + \frac{I^{(2)}_{\text{contrast}}}{I^{(2)}_{\text{ref}}} + \frac{I^{(3)}_{\text{contrast}}}{I^{(3)}_{\text{ref}}} + \cdots \tag{4}$$

This means that the sum of the normalized backscatter components need not necessarily be equal to the normalized backscatter of the whole signal.

Previous studies that used reference suspensions calculate the equivalent to the $\frac{I_{\text{contrast}}}{I_{\text{ref}}}$ ratio (Wang and Shung 1997, Sboros *et al* 2000a), while the present study aims to introduce the normalization of individual (nth) spectral components $\left(\frac{I^{(n)}_{\text{contrast}}}{I^{(n)}_{\text{ref}}}\right)$. It is evident that $I^{(n)}_{\text{ref}}$ is the linear backscatter intensity of the non-linearly propagated nth harmonic in the medium, while $I^{(n)}_{\text{contrast}}$ is probably partly the above linear backscatter intensity and partly the non-linear backscatter intensity of the contrast agent. Even though it is questionable if such a separation of the contrast backscatter is meaningful, this new approach to normalization should be capable of fulfilling the two goals ((a) and (b)) described above for such normalizations.

2.3. Reference materials

Measurements of backscatter coefficients of blood or other scattering materials have used the substitution technique introduced by Sigelmann and Reid (1973). The same principle has been used for the assessment of the backscatter properties of contrast agents (de Jong *et al* 1992, 1994b, de Jong and Hoff 1993, Frinking and de Jong 1998). In these papers the discrepancy between the results of different transducers, that overlap in the frequency domain, is sometimes large. Wang and Shung (1997) discuss the limitations in using plannar reflectors to characterize measurements from focused transducers and suggest the use of scattering particles as references.

The ideal reference material should provide strong scatterers (as strong as contrast agent scatterers) in order to provide individual scattering events well above noise levels. This will enable the concentration of the reference scatterers to be similar to the contrast microbubble concentration. In this case both transmit and scatter fields are perfectly simulated and direct comparisons of the scattering cross sections of the microbubbles to the reference scatterers can be made. An Orgasol® particle suspension similar to a blood mimicking fluid offers a suitable material for normalization purposes (Sboros *et al* 2000a). However, the very low echoes scattered from the Orgasol® particles did not allow visualization of individual scatterers at most machine settings, which suggested that the amplitude of those echoes was mostly below noise level and a high concentration must be used in order to achieve the required backscatter level. Therefore an Orgasol® suspension compromises the concentration of scatterers and introduces a small attenuation in the field that might affect scatter from non-linearly propagated ultrasound. Unfortunately it was impossible to find particles of similar size distribution to intravenous contrast agents, which would scatter echoes above the noise level of this system and satisfy the second (b) requirement of normalization mentioned above. Another approach was to use particles of a larger size, which still could be considered as Rayleigh scatterers. Although the comparison between such particles and contrast agent bubbles is not ideal, it is nevertheless a direct one between two Rayleigh scatterers. The size of a Rayleigh scatterer for the present experiment ought to be $\ll\lambda$ ($l \sim 345$ μm at 4.28 MHz which is the maximum transmit frequency).

In order to compare the above two approaches and also assess the normalization procedure as set in the previous section (goals (a) and (b)) two materials were tested as reference materials: (a) The suspension of Orgasol® scatterers of 5 μm diameter (Sboros *et al* 2000a) and (b) A gelatine suspension of Eccosphere®. Eccosphere® (New Metals & Chemicals Ltd, Essex, UK) comprises hollow glass spheres of a median diameter of 55 μm. One litre of sterile water was mixed with 0.5 g of Eccosphere®. A 200 ml batch of that suspension was added to 200 ml of boiling water mixed with 22 g of cooking gelatine. Gelatine was necessary in order to fix the particles in position since their density is 0.2 g ml^{-1}. Note that this gelatine was the only anechoic one among a wide range of gelatines (Agar, thrombin, etc). The resulting suspension was stirred for 30 min, introduced in the tank using a sieve of 90 μm aperture (model 200sbw.090, Endecotts Ltd, London, UK), which would consequently remove the larger spheres from the suspension. The suspension was then stored in a refrigerator for at least 6 h to solidify. The high temperature of the suspension prior to storage helped in avoiding bubble formation. These particles were the smallest size that would scatter signals sufficiently well to be detected individually by the scanner at all different combinations of settings. Finally, at these concentrations the attenuation of the Eccosphere® suspension was negligible and did not need to be compensated for.

Frames at a particular setting were also acquired every 30 min (first frame acquired at the start of acquisitions), to assess time variations of backscatter over time, in order to quantify

fluctuations of the consistency of the material in view or fluctuations of the performance of the system. The backscatter intensity was calculated for all acquired frames at the particular setting and was divided by the maximum backscatter intensity of all the series of experiments using the same material at this setting. The ratio was plotted versus time and a sixth-order polynomial was fitted to predict that ratio with time. The predicted ratio at a particular time multiplied with the backscatter intensity of the measurement at the same time gave way for time-compensating the backscatter intensity of interest.

2.4. Contrast agent

The contrast agent used was Definity (DuPont Pharmaceutical Co, Waltham, MA). The concentration of the agent in the tank was largely diluted to achieve visibility of single scattering events. This ensured that the assumption of negligible contrast attenuation was valid and that no interaction or multiple scattering occurs between microbubbles. This is important for non-linear scatterers like contrast bubbles that are also non-linear attenuators. Thus the total backscatter signal of a ROI was the sum of the signals of the individual particles. The potential to manually count the microbubbles in the field of view and calculate the average backscatter per microbubble is also conceivable. The average concentration used was approximately 23 bubbles per ml of suspension (sterile water) in the tank. The suspension was stirred for 30 s and the first triggered frame was then captured and stored in the PC. The velocity of the bubbles was small compared to the sweep speed and therefore their motion did not have any impact on the backscatter measurements. A sample of data was collected at all pulse lengths in order to decide which signals were suitable for second harmonic extraction and it was decided that 8-cycle pulses should be used to collect this preliminary set of data.

3. Results

3.1. Reference materials

Examples of reconstructed frames for Orgasol® and Eccosphere® materials are displayed in figure 3. The transmit frequency was 2.02 MHz, the pulse contained 2 cycles, and the MI was set at 0.5. The data were filtered using a passband window 600 kHz–9 MHz and then were reconstructed. The Orgasol® scatterers appeared more uniformly suspended when compared with the Eccosphere® type. The latter were more diluted and individual scatterers could be identified in the image. Orgasol® particles are smaller with lower impedance mismatch and therefore have a much lower scattering cross section than Eccosphere® particles. Thus they cannot be observed as individual scatterers and high-concentration suspensions were required to achieve detectable backscatter signals. Image reconstruction of the RF data was performed for each acquisition for visual inspection in order to detect and exclude the frames with artefacts.

Examples of calculated average backscatter intensity from the ROI are shown in figure 4 for the Orgasol® suspension and in figure 5 for the Eccosphere® suspension. Parts (a) of figures 4 and 5 referred to MI = 0.1 and parts (b) referred to MI = 0.6. The complete scattered signal, fundamental, 2nd and 3rd harmonic backscatter intensities were plotted versus frequency. The 2nd and 3rd harmonics show linear scatter of the non-linearly propagated ultrasound in the medium and the points were plotted in figures 4 and 5 only if a visible peak occurred at the particular frequency in the corresponding fast Fourier transform (FFT) plots. The 3rd harmonic signals were not apparent at MI = 0.1 in either materials. Note that

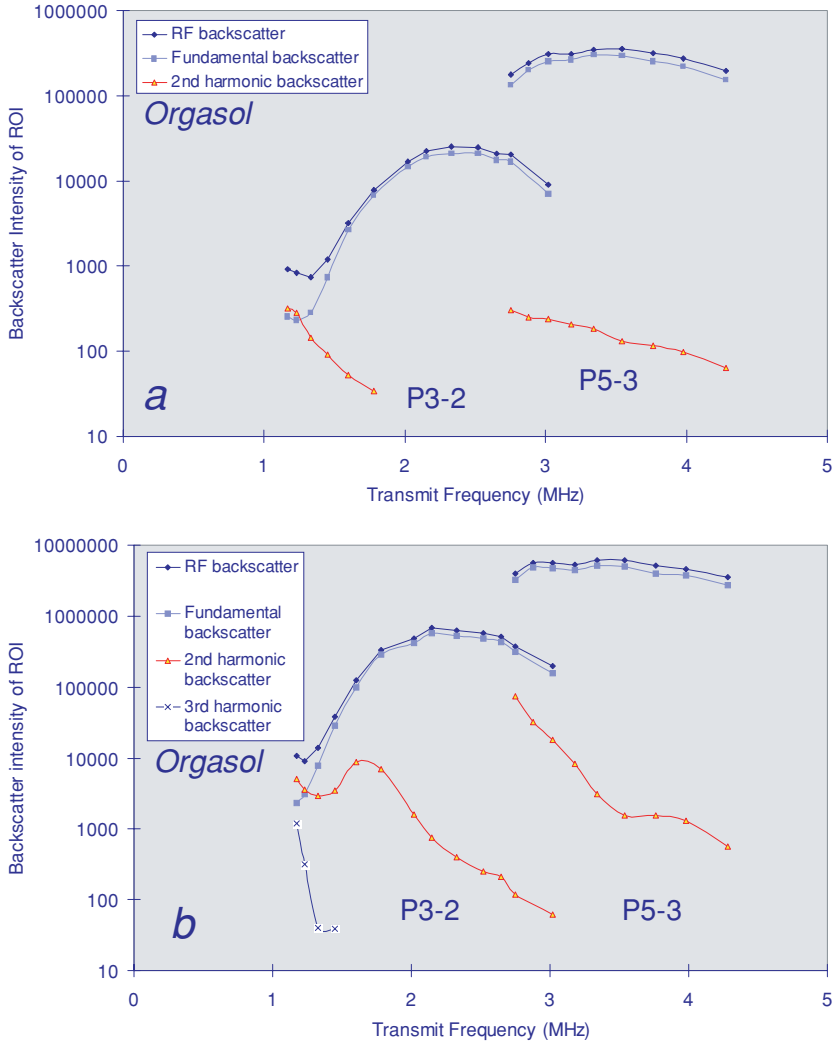

Figure 4. Backscatter intensity of the whole RF signal, fundamental, 2nd and 3rd harmonic components versus frequency for the Orgasol® suspension. Points were displayed when visually distinct peaks were visible when the whole signal was plotted in the frequency domain. The transmitted pulse was an 8-cycle one, and the MI was (a) 0.1 and (b) 0.6. The uncertainty of the intensity measurement does not exceed ±9% as specified by Sboros *et al* (2000a).

each point refers only to one acquisition. Even though the data were plotted on a logarithmic backscatter intensity scale, it is noticeable that the variability was relatively low. All the plotted lines followed a spectral behaviour with very low deviation. The spectral behaviour of the fundamental intensities (and obviously the whole RF signal), for example, of both materials, resembled those of the calibration shown in figure 2 (the peak negative pressures displayed in a linear scale). The lowest values of 2nd and 3rd harmonic intensities, in these figures, were just above the noise level of the two probes.

The range of transmitted acoustic pressures displayed a very low variation amongst different pulse lengths (<5%). Also, the transmit frequencies were very similar at all the

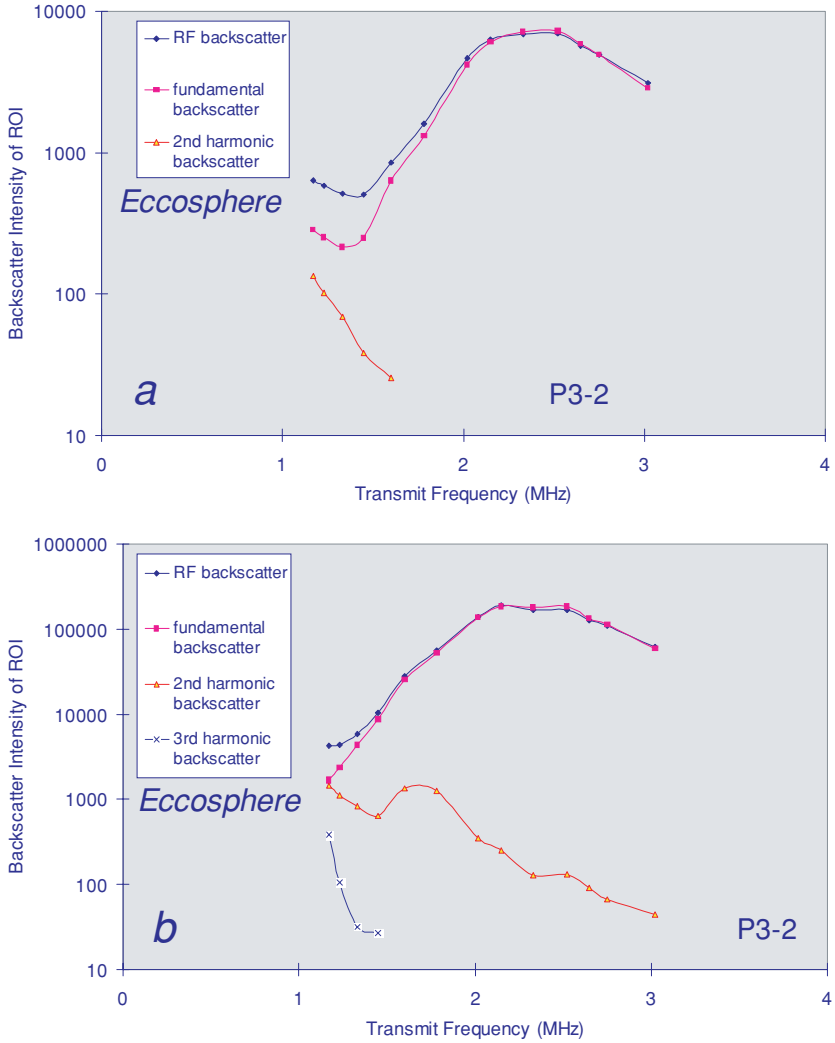

Figure 5. Backscatter intensity of the whole RF signal, fundamental, 2nd and 3rd harmonic components versus frequency for the Eccosphere® suspension. Points were displayed when distinct peaks were visible when the whole signal was plotted in the frequency domain. The transmitted pulse was an 8-cycle one, and the MI was (a) 0.1 and (b) 0.6. The standard deviation of the mean was less than ±3% for all the measurements of the intensity.

different pulse length settings (1.17–4.28 MHz). For four and more cycle pulses the range of centre frequencies at different pulse lengths was identical for all pulse lengths. This range narrowed for pulse lengths shorter than 4 cycles long (about 0.5 MHz for 2-cycle pulses). At a specific pulse length the calculation of the average backscatter intensity of the fundamental frequency component of the backscatter signals over different transmit frequencies, represents an estimation of the level of backscatter, and can be used for comparison between different pulse lengths. These values were plotted in figure 6 versus pulse length. Figure 6(a) refers to the Orgasol® suspension and figure 6(b) to the Eccosphere® suspension. The ratio of average backscatter intensity to the squared peak negative pressure, which is a measure of the

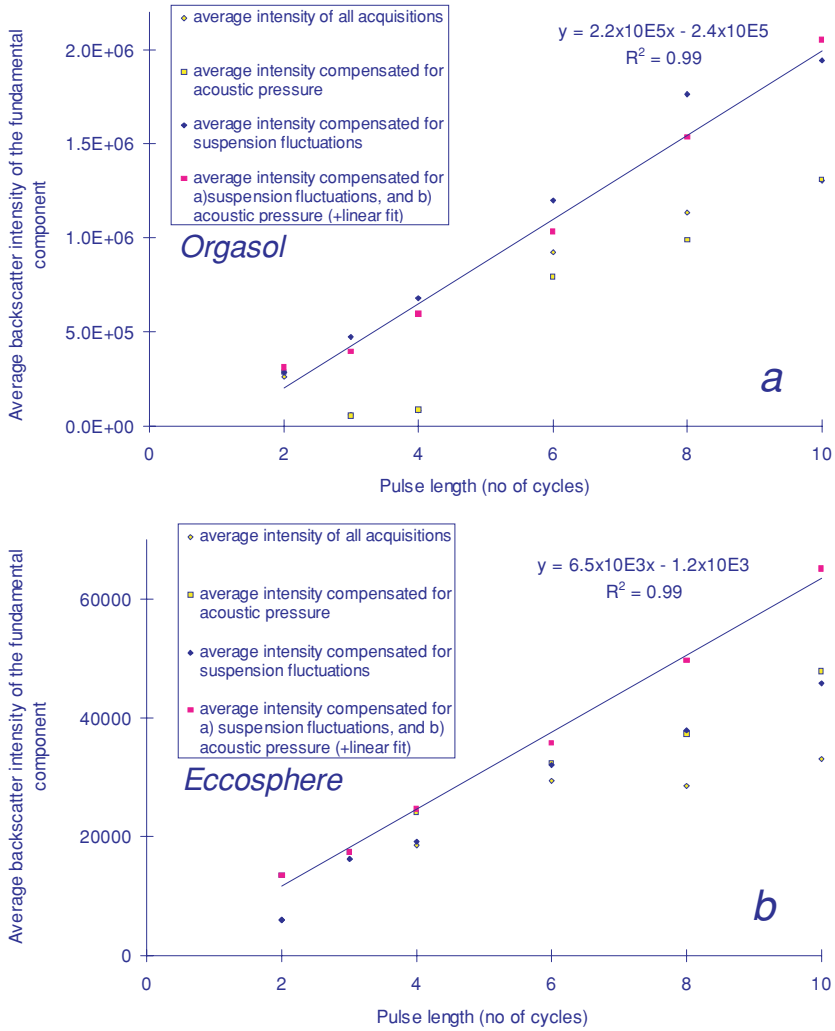

Figure 6. Average backscatter intensity versus pulse length. Four different calculations of intensity were displayed for comparison. The measured intensity, that which compensated for the time variability of the suspensions, one which normalized for the intensity of the transmitted pulse and one which both compensated and normalized. The latter showed a near-perfect linear relationship between backscatter intensity and pulse length for both the Orgasol® (a) and Eccosphere® (b) suspensions.

transmitted intensity, was included in this plot (average intensity compensated for acoustic pressure) in order to compensate for the variable sensitivity of the transducers over the used transmitted frequency spectrum.

As shown in figure 6, the small time fluctuations of both materials were compensated for effectively, and the backscatter level of both materials displayed a linear relationship between the backscatter intensity and the pulse length with very high regression coefficients. This relationship is expected for linear scatterers. The increase in pulse length increases proportionally the intensity of the transmitted pulse. Therefore, the scattered intensity from linear scatterers should be proportional to the increase of transmitted pulse length.

Compensating the average values of intensity with the square of peak negative pressure was equivalent to normalizing with the transmitted intensity, and showed that the true variability of the data was very low. The regression coefficient of the linear fit was greater than 0.99 for both materials. For the rest of this paper the backscatter intensity of both materials refers to the backscatter intensity compensated for time variations.

The FFT of the echoes showed that above 6-cycle pulses, the bandwidth was suitably narrow for extracting individual spectral components from those signals. The fundamental and harmonic components were clearly separated for the reference materials as well as the contrast agent suspension (figure 7). The ratio of backscatter intensity to the number of cycles was plotted versus peak negative pressure in figure 8(a) for the P5-3 probe, and in figure 8(b) for the P3-2 probe, for the Orgasol® suspension. The figures contain scattered data plots categorized in terms of frequency. Power fits showed high regression coefficients at a 2nd-order relationship between backscatter intensity and peak negative pressure which denotes the linearity of the scatterers in that material. Note that transmitted intensity has a 2nd-order relationship with the peak negative pressure. The trends provided a higher regression coefficient for the P5-3 probe. The results for the P3-2 probe were similar for the Eccosphere® suspension.

For a linear scatterer the increase in the number of cycles in each transmitted pulse was responsible for the linear increase of backscatter intensity (overall linear increase of transmitted energy). In a similar manner, an increase of wavelength, with the same number of cycles (i.e. decrease of frequency) gives a linear increase of backscatter intensity. The backscatter intensity was normalized for frequency and pulse length variations, as well as the peak negative pressure which expresses the spectral sensitivity of the probes (figure 2) and is reproduced in the patterns observed in figures 4 and 5 by the acquired data. The following formula provided an attempted normalization for the beam characteristics

$$nB = B \times f/cy \times p^2 \tag{5}$$

where nB was the normalized backscatter intensity, B the backscatter intensity, f the transmit frequency in MHz, cy the number of cycles in a pulse, and p the peak negative pressure in MPa as found in the calibration. The normalized backscatter intensity of the Eccosphere® suspension was plotted versus transmit frequency in figure 9(a), grouped in different transmitted peak negative pressures (probe P3-2). For the suspension of Orgasol®, the normalization produced figure 9(b) for the P3-2 probe.

The variability amongst different frequencies did not disappear in nB for either suspension of scatterers. However, the Eccosphere® suspension showed a very small variability within each frequency compared to the variability of the average nB (over acoustic pressure and pulse length) between different frequencies (figure 9(a)). In other words, the nB for each frequency did not vary much at different acoustic pressures and pulse length, which demonstrated that the normalization procedure suggested by equation (5) is efficient for the range of used acoustic pressures and pulse lengths, but not as efficient for the transmitted frequency. This low variability was not seen in the Orgasol® suspension in figure 9(b) apart from the three lowest transmit frequencies. The two materials were therefore compared in terms of median nB at each frequency. Figure 10 displays the ratio of the median of the Orgasol® suspension nB, at each frequency, to that of the Eccosphere® suspension. The result showed that the backscatter intensity of the Orgasol® suspension is four times that of the Eccosphere® suspension, except for the three lowest frequencies where the Orgasol® suspension backscatter was low and close to the noise level.

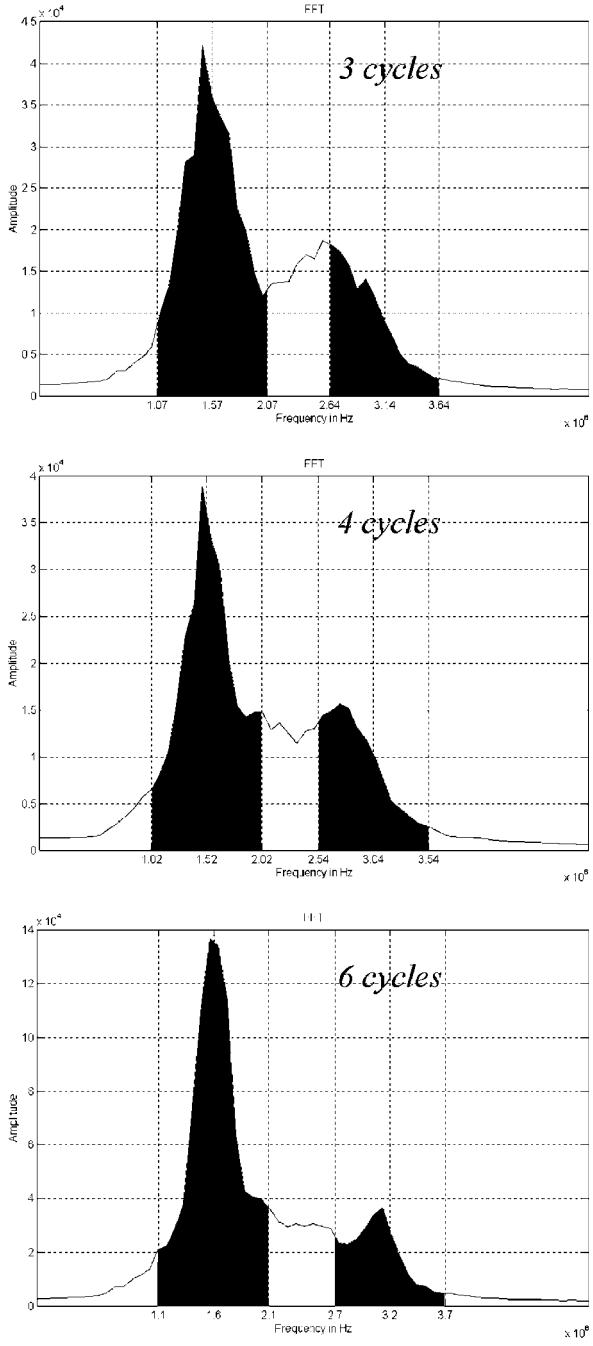

Figure 7. Received backscatter spectrum of Definity suspension at 1.57, 1.52 and 1.6 MHz transmit frequency at 3, 4 and 6-cycle pulses respectively. The black areas of the signal are those filtered out at either the fundamental frequency or the second harmonic. The graphs demonstrate a distinct peak of the signal at the fundamental frequency at all pulse lengths. However, the second harmonic peak becomes distinct at only the 6-cycle pulse length, while the 3 and 4-cycle pulse lengths demonstrate that the filtering process is not adequate for extracting the second harmonic from the backscattered signals.

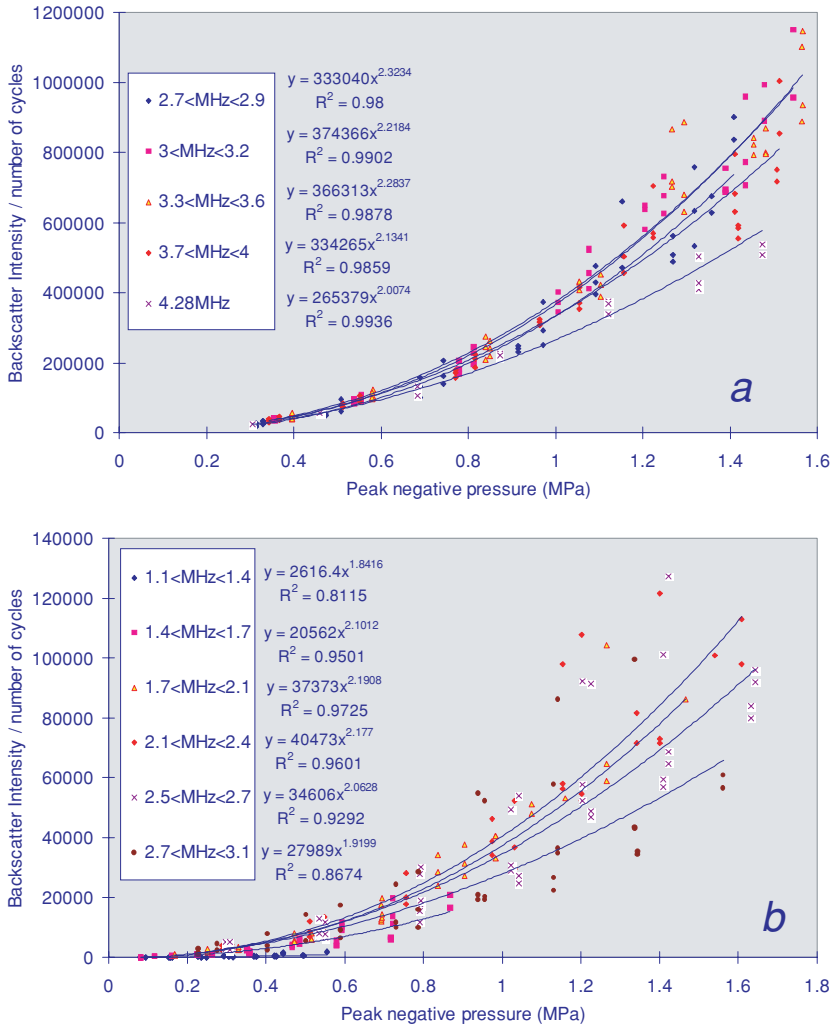

Figure 8. Ratio of backscatter intensity to pulse length plotted versus peak negative pressure (for pulse length > 6 cycles) for the suspension of Orgasol®. (a) probe P5-3 and (b) P3-2.

3.2. Contrast agent

The backscatter intensities of the Definity contrast suspensions for the four frequency windows described above were plotted versus transmit frequency in figure 11(a) and (b) for Mechanical Index equal to 0.2 and 0.6 respectively. Since only one measurement was taken for each combination of settings, the statistical uncertainty of that measurement is expected to be higher than ±20% due to the very small concentration of contrast microbubbles in suspension. However, because of the large number of settings that were used for measurements, the data plots in figure 11 display good patterns for qualitative conclusions. The RF and the fundamental frequency intensities follow a pattern similar to the transducer spectral sensitivity pattern (figure 2). This perhaps also applies for the 2nd harmonic intensity, although this sensitivity of the transducers was not assessed. These figures did not reveal any spectral behaviour that belongs to the contrast agent. Third harmonic signals were collected but only

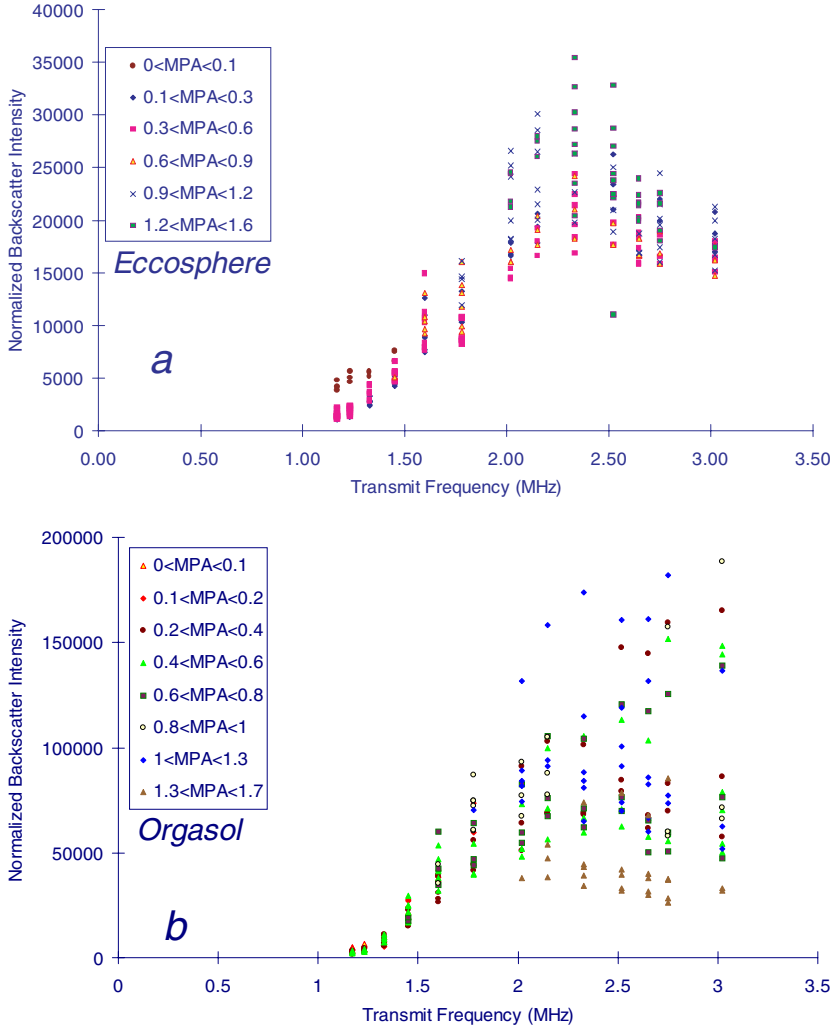

Figure 9. Normalized backscatter intensity, as compensated by equation (5), versus transmit frequency for the Eccosphere® suspension (a), and for the Orgasol® suspension (b).

for very low transmit frequencies. Therefore, a normalization process is essential in order to compensate for the characteristics of the transducer and allow information related to the contrast agent to be extracted.

The normalized backscatter of Definity was plotted versus transmit frequency in figures 12 and 13, for the Orgasol® and the Eccosphere® normalization respectively. Parts (a) and (b) of figures 12 and 13 refer to MI = 0.2 and 0.6 respectively. A dominant resonance between 1.5 and 2 MHz for MI = 0.2 was revealed from both normalization procedures. This peak seemed to be closer to 1.5 MHz for MI = 0.6. Harmonic and fundamental component visually seemed to match these peaks, demonstrating that the normalization procedure using reference materials is suitable for such measurements since fundamental and harmonic signals are collected at different spectral sensitivity ranges of the probes. Furthermore, the shape of the spectral behaviour of the normalized backscatter of the contrast agent was similar for harmonic and

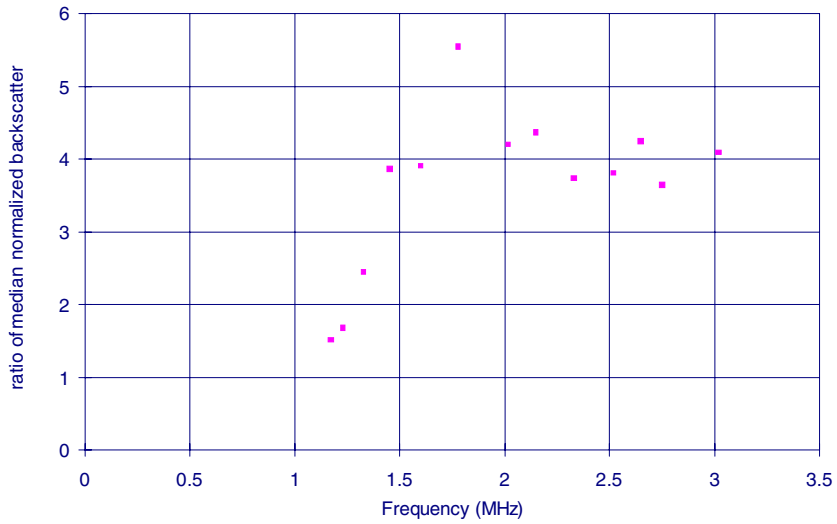

Figure 10. The ratio of the median of the Orgasol® suspension at each frequency to that of the Eccosphere® suspension is plotted against transmit frequency. The backscatter intensity of the Orgasol® suspension is fourfold of that of the Eccosphere® suspension, except for the three lowest frequencies where the Orgasol® suspension backscatter was located at the noise level. The ratio at 1.78 MHz is outside the general behaviour and is 5.5, which was due to the lower values of the Eccosphere® suspension at that frequency (figure 9(a)).

fundamental components which further validates the normalization approach. The smooth continuity of data from one probe to the other in figure 12 showed that the normalization approach can effectively compensate for different probes, even when the unnormalized data have completely different values at the same frequency (figure 11). Finally, the harmonic signal did not seem to give a more sensitive measurement in terms of normalized backscatter compared to the RF or the fundamental component normalized backscatter apart from the dominant resonance frequency.

4. Discussion

This paper presented an advanced version of an experimental ultrasonic system with expanded capabilities, compared to others used in *in vitro* experiments. The wide range of settings required an elaborate calibration and an expanded analysis tool. The evaluation of an experimental set-up is usually complete when a full calibration is performed and preliminary measurements demonstrate the functionality of the provided facilities. The present system is somewhat different since it also requires a normalization approach, which makes the normalizing materials central to the study. It is essential that these materials behave like suspensions of linear Raleigh scatterers which are fully explored in the literature, and ideally would act as a reference for comparison to contrast agents which have non-linear properties.

Second harmonic signals could be detected for the highest transmit frequency. In figure 4(b) the second harmonic was detected at 6 MHz for the P3-2 probe and at 8 MHz for the P5-3 probe (note that those figures are plotted versus transmit frequency). Third harmonic signals were also detected which denotes the high sensitivity of the system.

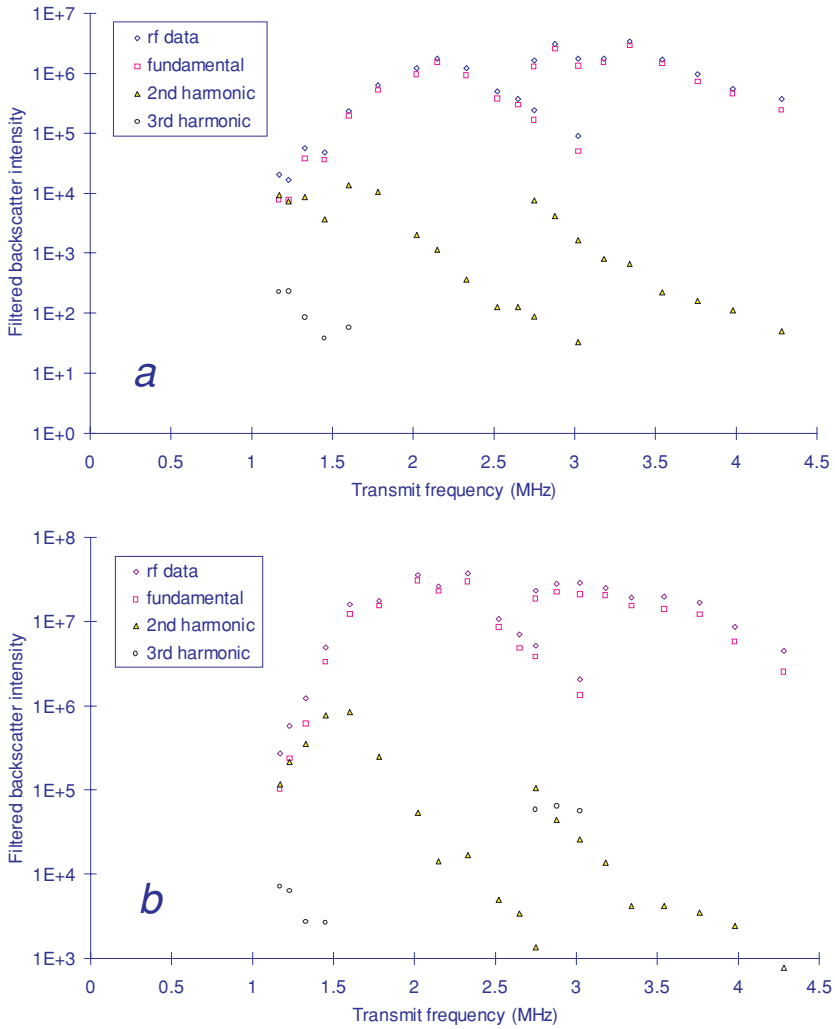

Figure 11. Backscatter intensity of the whole RF signal, fundamental, 2nd and 3rd harmonic components versus frequency for the Definity suspension. Points were displayed when distinct peaks were visible when the whole signal was plotted in the frequency domain. The transmitted pulse was an 8-cycle one and the MI was (a) 0.2 and (b) 0.6.

With the help of calibration, the backscatter intensity was normalized by means of equation (5). This simple arithmetical normalization was used in order to compensate for the different pulse characteristics. It also aimed to normalize for the spectral sensitivity of the probes as shown in figure 2 and reproduced by the data in figures 4 and 5. A dependency of the intensity on the 4th power of frequency (for the range of used frequencies), which is typical of Rayleigh scatterers (Morse and Ingard 1968) should then be expected in figure 9 from both scatterer suspensions. A 4th power fit did not express the dependence of the normalized data to frequency, apart from perhaps the Eccosphere suspension up to 2.3 MHz. Chen and Zagzebski (1996) measured a $f^{3.8\pm0.1}$ frequency dependence of Sephadex spheres (mean diameter 42 μm) below 5 MHz. After using a 90 μm pore sieve to insert the gelatine suspension of Eccosphere® into the tank, it was expected that the mean size of the particles

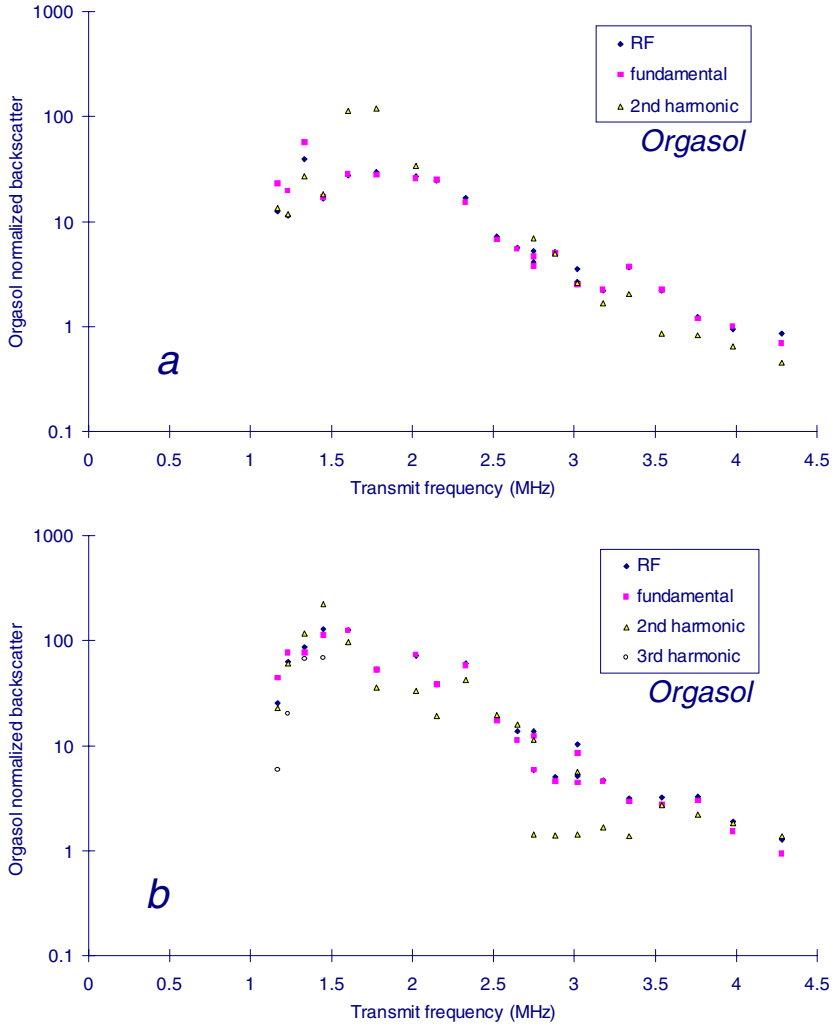

Figure 12. Orgasol® normalized backscatter intensity versus transmitted frequency at (a) 0.2 and (b) 0.6 MI. A peak is observed for all components (RF, fundamental, 2nd harmonic) between 1.5 and 2 MHz transmit frequency for MI = 0.2, while for MI = 0.6 the peak shifts just below 1.5 MHz.

would be lower than the initial 55 μm. The ratio of median backscatter between the Orgasol® and the Eccosphere® suspensions at each frequency, plotted in figure 10, was independent of frequency apart from the three lowest transmitted frequencies. This is because the Orgasol® provided very low signals close to noise levels and the sensitivity of the system is not adequate at the particular frequency range. This further demonstrated the similarity of the two linear scatterer suspensions and that the Eccosphere® scatterers could also be considered as Rayleigh scatterers. A high-order relationship between normalized backscatter and frequency occurred up to around 2 MHz (figure 8), but above that frequency a different behaviour was observed similar perhaps to the spectrum of figure 2.

This frequency dependence illustrates the limitation of the normalizing equation (5) in accounting for the parameters that affect the transmit and receive of the system. Figure 9(a)

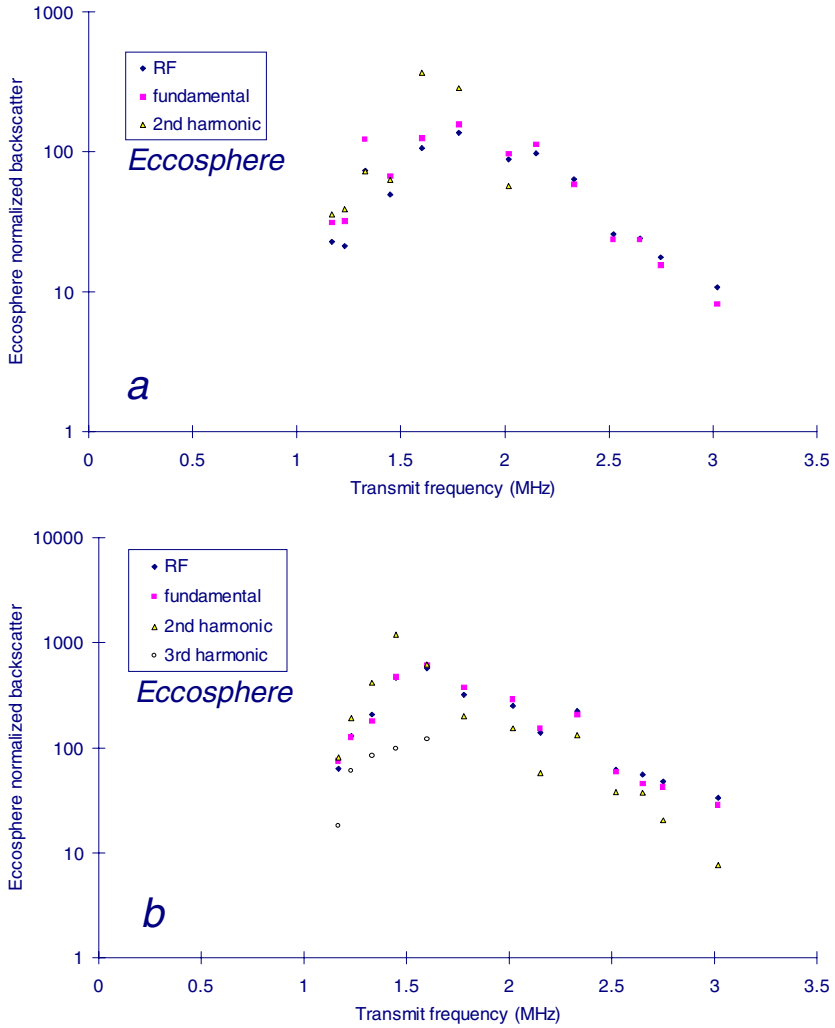

Figure 13. Eccosphere® normalized backscatter intensity versus transmitted frequency at (a) 0.2 and (b) 0.6 MI. A peak is observed for all components (RF, fundamental, 2nd harmonic) between 1.5 and 2 MHz transmit frequency for MI = 0.2, while for MI = 0.6 the peak shifts around 1.5 MHz.

showed that the arithmetic normalization, despite failing to fully normalize and hence reveal the scattering properties of the material at different frequencies (frequency dependence of scattering cross section of linear scatterers), was effective at most frequencies for the Eccosphere® suspension (figure 9(a)). This was demonstrated as a reduction of the variability of the normalized backscatter for different acoustic pressures and pulse lengths that were used at each transmit frequency. There is a noticeable difference in the scatter of the data between the Eccosphere® and the Orgasol® suspensions. The Orgasol® normalized data demonstrated a higher variability at each frequency compared to the Eccosphere®. Therefore equation (5) worked reasonably well in normalizing for acoustic pressure at each frequency for most frequencies, but was probably unable to compensate for other ultrasound field parameters such as beam width, focal range and focal depth. It is speculated that the variability of

response amongst different settings is caused primarily by the change of beam shape at different frequencies. This is concluded for the Eccosphere® suspension which provided a strong spectral pattern in figure 9(a). The Orgasol® suspension did not provide good compensation for settings by means of equation (5) within each frequency. It is speculated that the high concentration of scatterers of the Orgasol® suspension provided some attenuation with increasing frequency, not accounted for in equation (5).

Assessment of the parameters that affect the backscatter intensity values at different settings is difficult. It was shown in this paper that this requires a very detailed calibration across the whole of the ROI and using a normalization equation that emerges from simple physical arguments. The use of all the acquired data using both reference materials should be used. The new normalized backscatter approach was applied for the contrast agent at all spectral components and showed the effectiveness of this normalization procedure, despite the fact that the second requirement set in the data processing section, was not met exactly. Both harmonic and fundamental normalized components agreed on the location of a dominant resonance. Further evidence of successful normalization was the fact that the results from two probes overlapped (figure 12), when the initial shape of the data is taken into account (figure 11). It is therefore evident that the normalized data presented in figures 12 and 13 present spectral behaviour of Definity and the effect of the transducer characteristics are entirely removed. The peak spectral response around 1.5 MHz shown in the two figures is at a position of low sensitivity for the P3-2 probe (figures 2).

Even though at the level of a preliminary study, useful information was extracted for Definity, an elaborate and full range collection of data would lead to solid conclusions for the acoustical behaviour of the agent. The present set-up can be used to assess quantitatively the backscatter behaviour of contrast agents in the frequency domain and with the use of well-known reference materials the scattering cross section can be calculated at the fundamental and 2nd harmonic. The dependence of scattering cross section on acoustic pressure can also be assessed. Also using the facility of changing the pulse length of transmitted signals, the time domain information from backscatter signals can be studied elaborately to achieve better understanding of contrast microbubble oscillation motions. Full characterization of microbubble behaviour would be possible if further harmonics were available (3rd and 4th at least), which probably should be expected by future generations of transducers and would lead to a thorough understanding of the bubble motion in the ultrasonic field. By normalizing contrast backscatter, however, with reference materials that are linear scatterers not only accurate quantitative results can be produced, but also good assessment of the behaviour of a microbubble can be achieved.

5. Summary

A new system for the investigation of contrast agents was presented and evaluated in this paper. It provided a wide range of settings, transmit pulses between 2–11 cycles, a frequency range 1–4.3 MHz transmit and 1–8 MHz receive, and acoustic pressure 0.08–1.8 MPa. This allowed the extraction of the fundamental and 2nd harmonic components of the signal. Two scattering suspensions were used to normalize the echoes from contrast agent suspensions. In order to extract useful information from the contrast echoes, normalization should be performed with the assistance of such materials, which would compensate for the variations of the ultrasonic field at different settings. The use of the contrast agent Definity further showed that dominant resonance can be detected using the normalization procedure for both fundamental and harmonic modes.

References

Burns P N, Powers J E, Hope Simpson D, Uhlendorf V and Fritzsch T 1994 *Ultrasound Med. Biol.* **20** S73 (Abstract)
Chang P H, Shung K K and Levene H B 1996 *Ultrasound Med. Biol.* **22** 1205–14
Chen J F and Zagzebski J A 1996 *IEEE Trans UFFC* **43** 345–53
Chin C T and Burns P N 1997 *IEEE Ultrasonics Symp. Proc.* **2** 1557–60
Dayton P A, Morgan K E, Klibanov A L, Brandenburger G H and Ferrara K W 1999 *IEEE Trans UFFC* **46** 220–32
De Jong N, Ten Cate F J, Lancee C T, Roelandt J R T C and Bom N 1991 *Ultrasonics* **29** 324–30
De Jong N, Hoff L, Skotland T and Bom N 1992 *Ultrasonics* **30** 95–103
De Jong N and Hoff L 1993 *Ultrasonics* **31** 175–81
De Jong N, Cornet R and Lancee C T 1994a *Ultrasonics* **32** 447–53
De Jong N, Cornet R and Lancee C T 1994b *Ultrasonics* **32** 455–59
Frinking P J A and de Jong N 1998 *Ultrasound Med. Biol.* **24** 523–33
Frinking P J A, de Jong N and Cespedes E I 1999 *J. Ac. Soc. Am.* **105** 1989-1996
Krishna P D and Newhouse V L 1997 *Ultrasound Med. Biol.* **23** 453–9
Morgan K E, Dayton P A, Kruse D E, Klibanov A L, Brandenburger G H and Ferrara K W 1998 *IEEE Trans UFFC* **45** 1537–48
Porter T R and Xie F 1995 *Circulation* **92** 2391–5
Porter T R, Xie F, Kricsfeld D and Armbruster R W 1996 *J. Am. Coll. Cardiol.* **27** 1497–501
Sboros V, Moran C M, Anderson T, Pye S D, Macleod I C, Millar A M and McDicken W N 2000a *Ultrasound Med. Biol.* **26** 105–11
Sboros V, Moran C M, Anderson T and McDicken W N 2000b *Ultrasound Med. Biol.* **26** 807–18
Schrope B A, Newhouse V L and Uhlendorf V 1992 *Ultrason. Imaging* **14** 134–58
Schrope B A and Newhouse V L 1993 *Ultrasound Med. Biol.* **19** 567–79
Sigelmann R A and Reid J M 1973 *J. Ac. Soc. Am.* **53** 1351–55
Wang S H and Shung K K 1997 *IEEE Trans Biomed. Eng.* **44** 549–54